Palaeogeography, Palaeoclimatology, Palaeoecology 463 (2016) 60–67

Contents lists available at ScienceDirect

Palaeogeography, Palaeoclimatology, Palaeoecology

journal homepage: www.elsevier.com/locate/palaeo

Holocene changes in Antarctic Intermediate Water flow strength in the Southwest Atlantic

Ines Voigt [a,*], Cristiano M. Chiessi [b], Alberto R. Piola [c], Rüdiger Henrich [a]

[a] MARUM – Center for Marine Environmental Sciences and Faculty of Geosciences, University of Bremen, D-28359 Bremen, Germany
[b] School of Arts, Sciences and Humanities, University of São Paulo, São Paulo, Brazil
[c] Servicio de Hidrografia Naval and UMI-IFAECI, University of Buenos Aires, Buenos Aires, Argentina

ARTICLE INFO

Article history:
Received 15 December 2015
Received in revised form 7 September 2016
Accepted 26 September 2016
Available online 28 September 2016

Keywords:
Antarctic Intermediate Water (AAIW)
Southwest Atlantic
Holocene
North Atlantic Deep Water (NADW)
AAIW-NADW see-saw
Sortable silt

ABSTRACT

Antarctic Intermediate Water (AAIW) is an essential component of the Atlantic meridional overturning circulation (AMOC) contributing to balance the southward flow of North Atlantic Deep Water (NADW). However, the role of AAIW in Holocene abrupt climate changes remains poorly understood. Here we reconstruct changes in the flow strength of AAIW based on a high temporal resolution paleocurrent record from the Southwest Atlantic. Superimposed on a slight increase in AAIW strength at ~7 ka BP, a succession of millennial-scale AAIW variations is recognized in our paleocurrent records indicating a highly variable intermediate water circulation throughout the Holocene. Although variations in the strength and position of the Southern Westerlies Winds (SWW) are proposed to greatly influence the formation and circulation of AAIW, we cannot confirm such a potential SWW-AAIW linkage since our records of AAIW flow strength do not correlate to Holocene shifts of the SWW across the Atlantic. However, our data shows a good correspondence with abrupt variations in the AMOC with enhanced (reduced) northward advection of AAIW during periods of reduced (enhanced) NADW circulation. These results provide evidence for a Holocene AAIW-NADW see-saw. Thus, although the exact forcing mechanism remains unresolved, we suggest that Holocene perturbations in AAIW exerted a significant impact on the AMOC.

1. Introduction

In the modern ocean, Antarctic Intermediate Water (AAIW) is mainly formed in the Southeast Pacific and Southwest Atlantic (Piola and Gordon, 1989) (Fig. 1A). Around the tip of South America intermediate water is originated by subduction of cold and fresh Antarctic Surface Water across the Antarctic Polar Front, and by contributions of Sub-Antarctic Mode Water that originates from deep winter convection north of the Subantarctic Front (Garabato et al., 2009). AAIW is advected through the Drake Passage with the Antarctic Circumpolar Current and northward along the western slope of the Argentine Basin into the adjacent South Atlantic subtropical gyre (Fig. 1A). Thereby, the injection of cold and fresh AAIW into the South Atlantic subtropical gyre is thought to have important implications for the Atlantic heat and salinity budget, and hence can modulate the rate of North Atlantic Deep Water (NADW) formation (Rintoul, 1991; Graham et al., 2011). The AAIW that is modified to warm, salty varieties by air–sea fluxes and interior mixing in the Atlantic is thus an important component of the upper limb of the Atlantic meridional overturning circulation (AMOC) exerting a significant influence on the inter-hemispheric heat exchange (Lumpkin and Speer, 2007) (Fig. 1).

Abrupt changes in the northward flow of AAIW associated with AMOC reduction have been hypothesized for North Atlantic deglacial cold periods, Heinrich Stadial 1 and Younger Dryas (Marchitto et al., 1998; Zahn and Stüber, 2002; Rickaby and Elderfield, 2005; Came et al., 2008; Pahnke et al., 2008; Thornalley et al., 2011; Xie et al., 2012; Huang et al., 2014). However, controversy still persists as to whether the northward flow of AAIW is waxing or waning during Heinrich Stadial 1 and Younger Dryas.

The Holocene (11.7 ka BP to the present) has also been punctuated by a series of sub-millennial-scale North Atlantic cold events (Bond et al., 2001; Wanner et al., 2011a). Drift ice deposits recorded in North Atlantic sediments led to the suggestion that a significant part of the Holocene millennial-scale climate variability was driven by solar forcing, with changes in NADW formation as a possible amplifying mechanism that could contribute to their global imprint (Bond et al., 2001). High-resolution Holocene sedimentary records from the subpolar North Atlantic (Bianchi and McCave, 1999; Hall et al., 2004) indeed indicate a highly variable flow of Iceland Scotland Overflow Water (ISOW) (a precursor water mass of NADW) throughout the Holocene. However, these records do not provide an entirely consistent picture as times of reduced ISOW flow do not coincide with peaks in IRD deposition (Wunsch,

* Corresponding author.
E-mail addresses: ivoigt@marum.de (I. Voigt), chiessi@usp.br (C.M. Chiessi), apiola@hidro.gov.ar (A.R. Piola), henrich@uni-bremen.de (R. Henrich).

http://dx.doi.org/10.1016/j.palaeo.2016.09.018

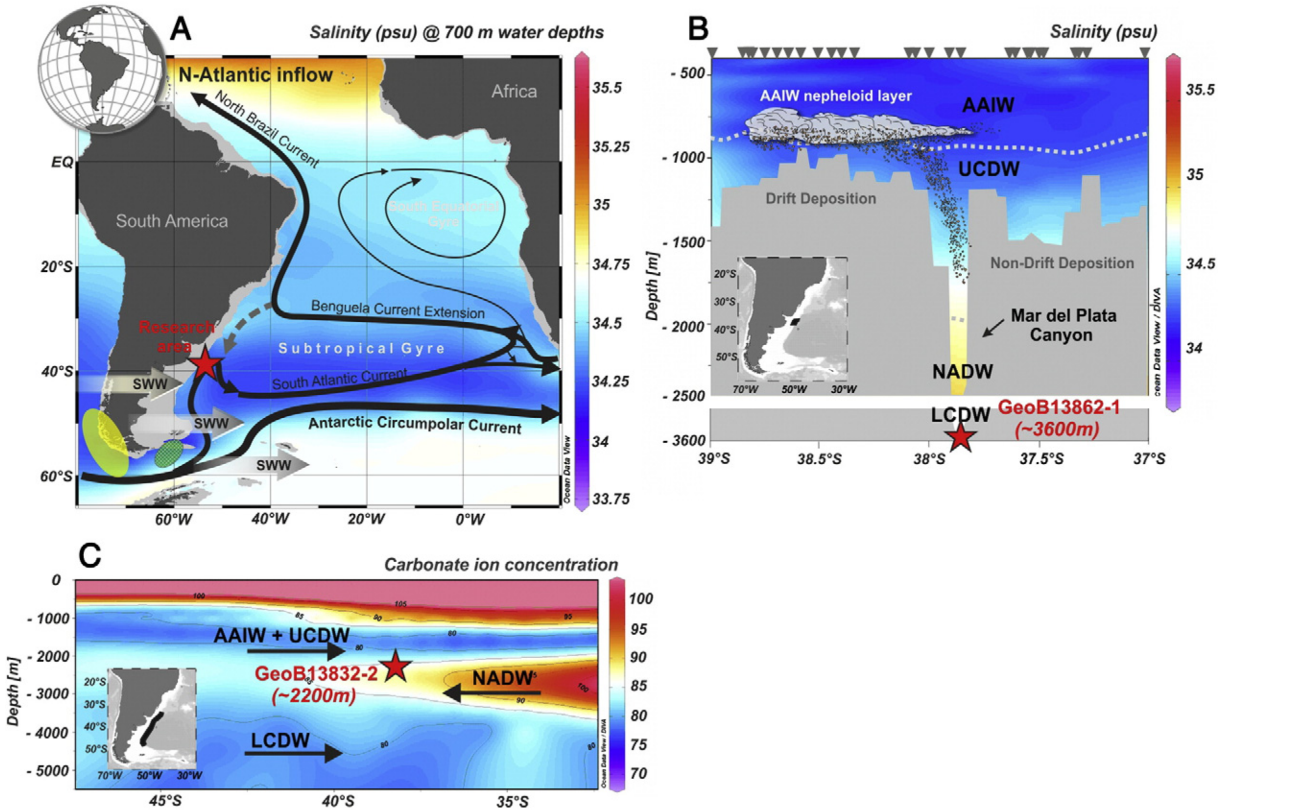

Fig. 1. A: Modern annual mean salinity (color shading) at 700 m water depth and schematic AAIW circulation (black arrows). The main AAIW source region is indicated by the yellow ellipse, and the region of strong AAIW mixing by the green ellipse. Grey arrows mark the prevailing Southern Westerly Winds (SWW). B: Along-slope salinity (color shading) section in the vicinity of the Mar del Plata Canyon (adapted from Voigt et al. (2013)). By crossing the Mar del Plata Canyon the suspended material of the AAIW nepheloid layer is released into the canyon which results in rapid and continuous deposition of sediments in the canyon. The red star indicates the location of core GeoB13862-1 whose terrigenous sortable silt fraction (10–63 μm) is used in this study to reconstruct paleo-variability of AAIW. C: Modern carbonate ion (CO_3^{2-}) concentration in the Southwest Atlantic. The red star indicates the location of core GeoB13832-2 ideally situated to monitor past changes of the interface between southern sourced waters (i.e., AAIW + UCDW) and northern sourced waters (i.e., NADW). AAIW – Antarctic Intermediate Water; NADW – North Atlantic Deep Water; UCDW – Upper Circumpolar Deep Water; LCDW – Lower Circumpolar Deep Water. Figures were prepared using Ocean Data View (http://odv.awi.de).

2000; Hall et al., 2004). Accordingly, there is still a clear need to determine the forcing mechanisms for abrupt Holocene changes in the AMOC. Model simulations demonstrate that initial changes in AMOC strength can be related to perturbations in AAIW, thus supporting the hypothesis of a quasi-synchronous AAIW-NADW coupling under Holocene boundary conditions (Graham et al., 2011). However, high temporal resolution climate archives that confirm a possible AAIW-NADW linkage during the Holocene are sparse (Arz et al., 2001), rising a major question: To what extent was the AMOC affected by past perturbation in AAIW overturning circulation throughout the Holocene?

Here, we present a high temporal resolution Holocene paleocurrent record of AAIW flow strength based on an unconventional site in the Southwest Atlantic. Our data suggest millennial-scale changes in the flow strength of AAIW with a potential link to changes in NADW fluctuations during the Holocene.

2. Regional setting

The Southwest Atlantic is a key location in the global ocean conveyor belt (Fig. 1). Different water masses formed in remote areas of the world flow across the Southwest Atlantic and generate a highly complex vertical stratification structure. In the upper ocean, this structure is dominated by the encounter of the southward flowing Brazil Current and the northward flowing Malvinas (Falkland) Current that produces one of the most energetic regions of the world ocean, the Brazil-Malvinas Confluence (BMC) (Peterson and Stramma, 1991; Piola and Matano, 2001). In the deep ocean, the vertical stratification is dominated by contributions from intermediate- and deep water masses including (from top to bottom) Antarctic Intermediate Water (AAIW, ~500–1000 m), Circumpolar Deep Water (CDW, ~1000–4000 m) and Antarctic Bottom Water (AABW > 4000 m) (Stramma and England, 1999) (Fig. 1C). By penetrating into CDW, North Atlantic Deep Water (NADW, 2000–3000 m) vertically divides this water mass into two layers referred to as the upper CDW (UCDW) and the lower CDW (LCDW).

In this region strong contour currents shape the continental margin by eroding, transporting and depositing sediments. These currents generate various depositional and erosive features, which together are referred as a Contourite Depositional System (CDS) (Hernandez-Molina et al., 2009). Sedimentation processes within the CDS are primarily controlled by northward-flowing Antarctic water masses, that on the upper slope is dominated by AAIW (Hernandez-Molina et al., 2009; Preu et al., 2013) (Fig. 2). The Mar del Plata Canyon at the continental margin off northern Argentina intersects this CDS (Fig. 1B, 2B). The canyon does not present an obvious connection to the shelf or an on-shore river system (Krastel et al., 2011), and is therefore isolated from shelf-originated down-slope processes (Voigt et al., 2013) (Fig. 2).

Measurements of high turbidity which are part of the world ocean nepheloid layer composition database assembled by the Lamont-Doherty Earth Observatory indicate a very pronounced AAIW nepheloid layer (Voigt et al., 2013) (Fig. 2A). In addition, the OCCAM Global Ocean Model (Gwilliam, 1996) show flow velocities of ~15–20 cm/s at 1000 m water depth. Directly beneath the high velocity core of AAIW, toward the AAIW/UCDW interface, sediments from the nepheloid layer deposit and accumulate leading to the formation of drift deposits south of the Mar del Plata Canyon (Preu et al., 2013) (Fig. 2B). In contrast, modern sediments directly north of the canyon do not reflect

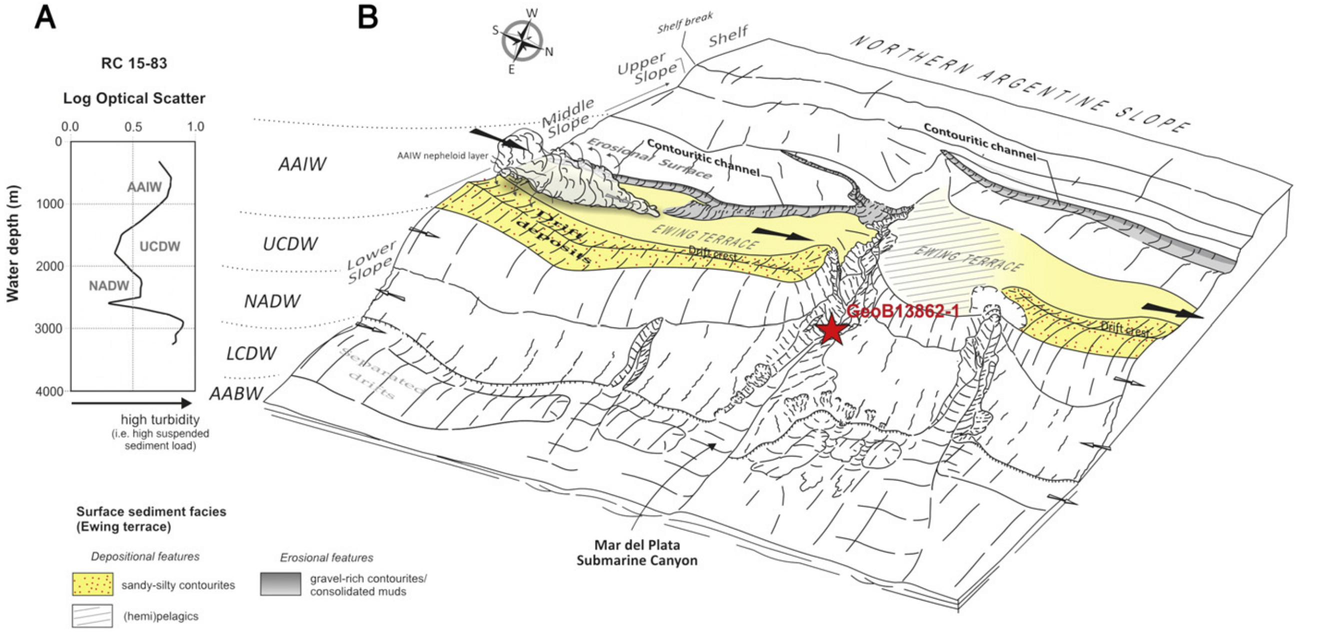

Fig. 2. A: Turbidity depth profile (Lamont-Doherty Earth Observatory) south of Mar del Plata Canyon. High values at intermediate depth suggest a very pronounced intermediate nepheloid layer testifying the strong current activity in the depth range of AAIW. B: Morpho-sedimentary map of the NE Argentine margin (adapted from Preu et al., 2013 and Voigt et al. (2013)) shows that the Mar del Plata Canyon is incorporated into a Contourite Depositional System. Yellow-colored surfaces indicate the Ewing terrace that is located at the lower boundary of AAIW. Voigt et al. (2013) argue that the presence of the Mar del Plata Canyon decreases the transport capacity of AAIW, in particular of its deepest portion that is associated with the nepheloid layer, which in turn produces a significant change in the contourite deposition pattern around the canyon. Accordingly, drift deposits occur south of the Mar del Plata Canyon, but are missing directly north of it. Surface sediment facies along the Ewing terrace were drawn after Bozzano et al. (2011). The red star indicates the location of core GeoB13862-1, investigated in this study. AAIW – Antarctic Intermediate Water; UCDW – Upper Circumpolar Deep Water; NADW – North Atlantic Deep Water; LCDW – Lower Circumpolar Deep Water; AABW – Antarctic Bottom Water.

such current-controlled sedimentation, but are characterized by (hemi)pelagic sedimentation (Bozzano et al., 2011) (Fig. 2B). Hence, a marked change in contourite drift construction occurs around the Mar del Plata Canyon, which indicates a dramatic decrease of the flow strength between the southern and northern sides of the canyon. Voigt et al. (2013) thus argued that the canyon alters the circulation of the northward-flowing AAIW, in particular its deepest portion associated with the nepheloid layer which primarily influences the depositional pattern around the Mar del Plata Canyon (Preu et al., 2013), and proposed that the canyon acts as a sink for enhanced accumulation of sediments (Fig. 1B). Indeed, the deposits inside the canyon reveal sediment characteristics similar to drift deposits. More precisely, the dominance of the sortable silt fraction (10–63 μm) over other particle sizes in the canyon (Voigt et al., 2013) indicates a response to hydrodynamic processes (McCave et al., 1995) and strongly supports the hypothesis of current-controlled sedimentation in the Mar del Plata Canyon. Accordingly, sediments transported within AAIW were gradually released into the canyon and produced a continuous ~750 cm long Holocene record, thereby providing a high temporal resolution climate archive suitable to study the paleo-AAIW variability throughout the Holocene (Voigt et al., 2013; 2015). In this study we use grain-size parameters (e.g., sortable silt paleo-current flow proxies) (McCave et al., 1995) from the canyon sediments to infer past changes in AAIW flow speed in the Southwest Atlantic.

We further applied the *Globigerina bulloides* dissolution index (BDX), which has been shown to precisely detect calcite dissolution within deep-sea sediments (Henrich et al., 2004). In the modern ocean, the core site investigated for BDX (i.e., GeoB13832-2) is situated at the interface between southern (AAIW/UCDW) and northern sourced water masses (NADW) (Fig. 1C). Because NADW is slightly supersaturated with respect to calcite it allows good preservation of calcareous sediments. In contrast, the overlying AAIW/UCDW has a lower carbonate ion concentration than NADW fostering dissolution of calcareous sediments (Fig. 1C). We use the BDX to determine vertical shifts of the interface between AAIW/UCDW and NADW, and the relationship between these shifts and AAIW current strength.

3. Material and methods

We studied marine gravity cores GeoB13832-2 and GeoB13862-1 recovered in the Mar del Plata Canyon, Southwest Atlantic (Table 1) (Figs. 1, 2). The cores were collected during RV Meteor cruise M78/3 (Krastel et al., 2012).

3.1. Age model

The ^{14}C-based age model for both cores was previously published by Voigt et al. (2013, 2015). The age model for the Holocene section of GeoB13862-1 is based on seven Accelerator Mass Spectrometry (AMS) ^{14}C dates determined on monospecific samples of the planktonic foraminifer *Globorotalia inflata* (>150 mm fraction). Stratigraphic correlation between the core GeoB13862-1 and core GeoB13832-2 was based on ^{14}C ages and X-ray fluorescence (XRF) down-core records of Ca and Fe (for details see Voigt et al. (2013), Fig. 3 shows age control points for cores GeoB13862-1 (light grey circles) and GeoB13832-2 (dark grey circles). The radiocarbon dates were calibrated with CALIB 6.0 software (Stuiver and Reimer, 1993) applying the Marine09 calibration curve (Reimer et al., 2009) and no ΔR. The age model was obtained by linear interpolation between calibrated ages. Fig. 3 shows the age control points used to produce the age models of both cores.

Table 1
Location of sediment cores used in this study.

Cruise	Core	Latitude	Longitude	Water depth (m)	Recovery (cm)
M78/3a	GeoB13832-2	37°57.07′ S	53°50.12′ W	2205	556
M78/3b	GeoB13862-1	38°01.06′ S	53°44.42′ W	3588	1016

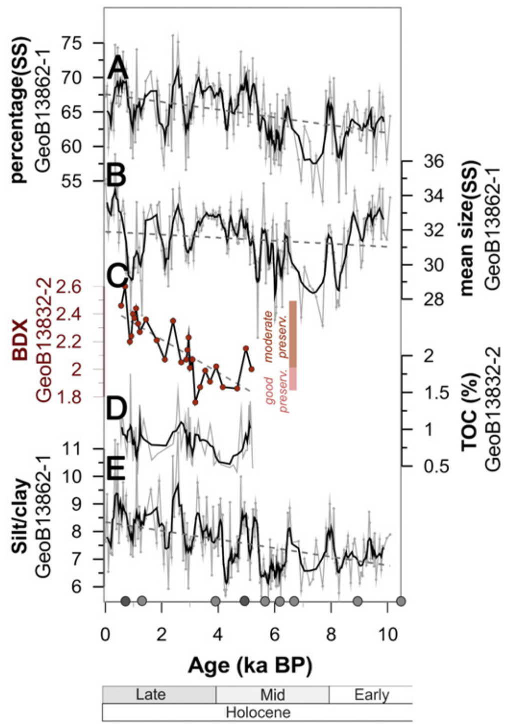

Fig. 3. Holocene paleocurrent records from the Southwest Atlantic. A: Percentage$_{(SS)}$ of core GeoB13862-1. B: Mean$_{(SS)}$ of core GeoB13862-1. C: *Globigerina bulloides* dissolution index (BDX) of core GeoB13832-2. D: Total organic carbon (TOC, wt%) of core GeoB13832–2. E: Silt/clay ratio of core GeoB13862-1 (clay defines the fraction below 2 < μm). Age control points for cores GeoB13862-1 (light grey circles) and GeoB13832-2 (dark grey circles) are shown at the bottom of the panel (Voigt et al., 2013). A, B, D and E were plotted with a five-point running average (black lines) on top of the original data (grey lines), while C shows a linear regression.

3.2. Sortable silt paleocurrent proxy

We applied sortable silt paleo-current flow proxies (i.e., sortable silt mean size (mean$_{(SS)}$) and percentage (percentage$_{(SS)}$); (McCave et al., 1995)) to reconstruct relative changes in intermediate-depth contour-current strength, i.e., the AAIW flow strength. Both parameters refer to the fraction of the sediment (i.e., terrigenous 10–63 μm) whose size sorting varies in response to hydrodynamic processes, where higher values reflect stronger near-bottom flow and vice versa (McCave et al., 1995). Grain-size distributions of the terrigenous fraction were measured with a LS 13320 Laser Diffraction Particle Size Analyzers, resulting in 116 size classes from 0.04 to 2000 μm. Laser diffraction particle sizing has been shown to yield high-precision data that accurately reflect even small changes in the mixing proportion of sediments (Goossens, 2008; Jonkers et al., 2009), although measurements might be biased due potential particle shape effects (McCave et al., 2006). The technique is thus well suited for paleoceanographic reconstructions. In order to isolate the terrigenous fraction (i.e., organic carbon-, carbonate-, and opal-free), several pretreatment steps were undertaken as described in Mulitza et al. (2008).

3.3. Globigerina bulloides dissolution index and total organic carbon

The determination of the BDX is based on scanning electron microscope ultrastructural investigation of planktonic foraminifera *Globigerina bulloides* (for methods, see Volbers and Henrich, 2002). The amount of total organic carbon (TOC, wt%) in core GeoB13832-2 was measured with a LECO CS-300 element analyzer to evaluate dissolution generated by changes in the vertical flux of organic carbon.

4. Results

4.1. Sortable silt paleocurrent proxy

Our paleocurrent record of GeoB13862-1 indicates the presence of a highly variable AAIW flow throughout the Holocene (Fig. 3). The mean$_{(SS)}$ varies between ~28 and 34 μm, while the percentage$_{(SS)}$ varies from 52 to 75% (Fig. 3A,B). A pronounced minima in mean$_{(SS)}$ and percentage$_{(SS)}$ occurs at around at ~7 ka BP, whereas both parameter start to slightly increase after ~7 ka BP. Additionally, both paleocurrent parameters show a high level of coherence and are clearly dominated by a short-term variability, together with the silt/clay ratio (Fig. 3A,B,E).

4.2. Globigerina bulloides dissolution index and total organic carbon (TOC)

The BDX record is clearly dominated by a long-term trend over the last 5.5 kyr as estimated by a linear regression. BDX values increase from 1.9 at the mid- Holocene to 2.6; i.e., preservation reduces during the late Holocene (Fig. 3C). The observed change in BDX appears not to be related to the changes of TOC because of constant TOC concentrations of ~1%.

5. Discussion

The mean$_{(SS)}$ and percentage$_{(SS)}$ have been argued to be proxies for near-bottom paleocurrent strength, where higher values reflect stronger near-bottom flow, and vice versa (McCave et al., 1995). The question whether the grain-size parameters in the Mar del Plata Canyon are related to the strength of circulation within the AAIW cell is of fundamental relevance for the interpretation of our mean$_{(SS)}$ and percentage$_{(SS)}$. The depositional background of the canyon is very complex because of the various flow and transport regimes of deep water masses along the Argentine margin: Hence, changes in grain-size parameters could reflect different sources of sediment associated with the distinct flow regimes of northern- and southern sourced water masses and/or additional sediment supply by tidal current processes or down-canyon transport processes (i.e. turbidites) may disturb or overprint the signal of AAIW bottom current strength.

Although submarine canyons constitute an important and unique setting for focusing tidal energy, it is questionable if tidal current reworking can occur in submarine canyons without any obviously connection to the shelf. Since the Mar del Plata Canyon is wholly confined to the continental slope, the area of the shelf-slope break remains still well developed, and thus forms an important physiographic boundary of tidal (bottom) currents (Shanmugam, 2003). Further, a study of the dynamics, dispersal, and accumulation of sediment deposits in the Mar del Plata canyon (Voigt et al., 2013) demonstrate that Holocene deposits in the canyon indicate no systematic turbidite deposits, which exclude a nearby source on the shelf and/or adjacent continent for the sediments deposited in the canyon. Voigt et al. (2013) thus suggested that (lateral) current-controlled transport appear to be the dominant process influencing the sedimentation pattern in the canyon and argued that the canyon alters the circulation of the northward-flowing AAIW. Particularly, the deepest portion of the AAIW associated with a nepheloid layer induces a rapid and continuous deposition of terrigenous coarse-silt material (i.e., sortable silt). We propose that this layer is a major contributor to the sediments deposited in the canyon at remarkably high sedimentation rates of ~150 cm/kyr during the Holocene. A significant change in contourite drift construction that occurs along the Ewing terrace (Fig. 2B) further supports a possible interaction of the canyon with the northward-flowing AAIW, which primarily influences drift deposition around the Mar. del Plata Canyon (Preu et al., 2013). Accordingly, in such highly energetic current regions as the Southwest Atlantic, where contour currents rework significant amounts of sediment, a submarine canyon can potentially act as a sink for enhanced accumulation of sediments, holding a great potential as a climate archive (Voigt et al., 2013, 2015). Thus, we consider the variation in $mean_{(SS)}$ and $percentage_{(SS)}$ to be mainly controlled by variability in the intensity of AAIW bottom current strength. Accordingly, higher $mean_{(SS)}$ and $percentage_{(SS)}$ are considered to be evidence for stronger AAIW bottom current strength and vice versa. Hence, our mean(ss) indicate an increase in AAIW bottom current strength at ~7 ka, with weaker current flow during the early/mid Holocene if compared to the late Holocene (Fig. 3). Superimposed on the increase at ~7 ka BP, a succession of millennial-scale AAIW variations is recognized in our paleocurrent record indicating a highly variable intermediate water circulation throughout the Holocene (Fig. 3).

Variability in BDX is commonly associated with a changing corrosiveness of the bottom water. The increase in AAIW bottom current strength at ~7 ka BP is followed by a long-term decrease in calcite preservation at the depth of core GeoB13832-2 (i.e. ~2 km) (Fig. 3C). This likely argues for a coupling, because only the geostrophic currents should be capable of influencing both the physical flow and the geochemical properties of deep waters. However, several processes as such as exposure time at the sediment-water interface and/or porewater dissolution driven by organic can bias the BDX degradation (Emerson and Archer, 1990; Jahnke and Craven, 1994). The exposure time at the sediment-water interface was relatively short owing to the high sedimentation rates in the Mar del Plata Canyon (Voigt et al., 2013). Further, changes in the flux of organic matter that might have overprinted the BDX can be neglected due to the relatively constant TOC content in GeoB13832-2 (Fig. 3D). The change in BDX thus suggests that calcite preservation varied significantly during the mid-to late Holocene, which is most probably associated with a changing corrosiveness of the bottom water bathing core site GeoB13832-2. Thus, we postulate that the reduced preservation of calcite reflects an increased influence of more corrosive AAIW/UCDW at the expense of NADW at this water depth most probably related to a slight deepening of the interface between southern- and northern sourced waters from mid- to late Holocene.

5.1. Forcing of Holocene AAIW variability

Model studies propose that SWW would induce ocean cooling and freshening by favoring the northward Ekman freshwater transport; with increase AAIW renewal during periods of intensified SWW (Ribbe, 2001; Saenko and Weaver, 2001) and/or poleward shifted SWW (Oke and England, 2004). Hence, variations in the strength/position of the SWW and associated ice-ocean freshwater fluxes are proposed to greatly influence the formation and circulation of AAIW. So far, there is surprisingly little systematic knowledge about sub-millennial-scale variability of the SWW during the Holocene (Fletcher and Moreno, 2012; Kilian and Lamy, 2012). However, evidence for temporal and spatial evolution of the SSW across the South Atlantic comes from a north-south transect of high-temporal resolution planktonic foraminiferal oxygen isotope records that reveal Holocene migrations of the BMC (Voigt et al., 2015), a highly sensitivity feature for changes in the strength and position of the SWW (Sijp and England, 2008; Lumpkin and Garzoli, 2011) (Fig. 4G). Because the SWW reconstruction from Voigt et al. (2015) is based on the same sediment core as our paleocurrent data (i.e. GeoB13862-1), we are in a unique position to neglect possible age model uncertainties. The oxygen isotope record of GeoB13862-1 shows high-amplitude (up to 2‰) sub-millennial-scale changes throughout the Holocene, clearly indicating alternated phases of Brazil Current and Malvinas (Falkland) Current influence as representative of sub-millennial-scale meridional shifts of the BMC. Accordingly, Voigt et al. (2015) propose a gradual orbitally forced ~1–1.5° poleward movement of the Atlantic SWW during the early to mid-Holocene until ~5 ka BP, and no discernible long-term trend afterwards. The data further provide evidence for sub-millennial-scale changes in the latitudinal position of the SWW of the order of 1°. However, the timing of SWW

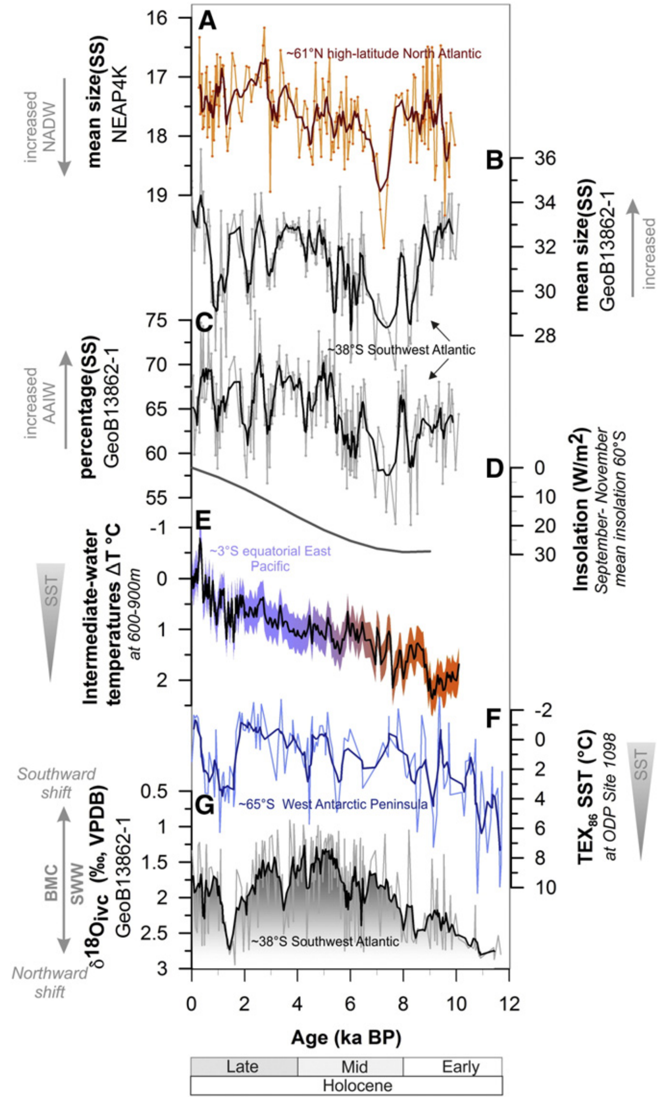

Fig. 4. Orbital to millennial-scale variability in the bottom current strength of AAIW compared with other Holocene climate records. A: $Mean_{(SS)}$ of core NEAP4K (Hall et al., 2004). B: $Mean_{(SS)}$ of core GeoB13862-1. C: $Percentage_{(SS)}$ of core GeoB138621. D: Austral spring (September–November) mean insolation at 60°S, plotted as deviations from present-day mean (Berger and Loutre, 1991; Renssen et al., 2005). E: Changes in intermediate-water temperatures in the eastern equatorial Pacific at 600 to 900 m (Rosenthal et al., 2013). F: TEX_{86}-derived sea surface temperatures (SST) in the sub-Antarctic Pacific (Shevenell et al., 2011) G: Ice volume corrected *Globorotalia inflata* $\delta^{18}O$ ($\delta^{18}O_{ivc}$) record of GeoB13862-1 indicating meridional shift of the Brazil-Malvinas Confluence (BMC) (Voigt et al., 2015). A, B, C, F and G were plotted with a five-point running average (black lines) on top of the original data (grey lines). Note that plots E and F have reversed y-axis.

change at ~5 ka BP is inconsistent with the abrupt changes in our paleocurrent record at ~7 ka BP (Fig. 4B,C,G).

Hence, our data do not support a potential SWW-AAIW linkage as suggested from climate model studies (Ribbe, 2001; Saenko and Weaver, 2001; Oke and England, 2004). At least, we exclude the SWW as a potential driver for Holocene changes in AAIW formation and circulation in the western Atlantic sector of the Southern Ocean.

In general, on sub-millennial-scale timescales it is still difficult to assess the exact forcing mechanisms behind changes in AAIW circulation strength since Holocene reconstructions of the Southern Hemisphere climate are controversial because the available records show strong regional complexity (Mayewski et al., 2004; Wanner et al., 2011a). However, a considerable change in the seasonal and latitudinal distribution of insolation characterized the period between ~7 ka BP and present-day in the high-latitudes of the Southern Hemisphere (Berger and

Loutre, 1991; Renssen et al., 2005) (Fig. 4D). The minor increase in AAIW strength at ~7 ka might therefore be associated with a decrease in austral winter-spring insolation at 60°S (Renssen et al., 2005) which would lead to anomalously cold conditions in regions of AAIW formation. The sensitivity of AAIW current strength to 60°S winter-spring insolation might be associated with enhanced water mass formation in late austral winter and early spring when low air temperatures, increased sea-air turbulent heat fluxes and variations in sea-ice extent act to deepen the winter mixed layers as a result of enhanced convection in the formation region west of the Antarctic Peninsula (e.g. Garabato et al., 2009). The similarity between changes in winter insolation at 60°S and our paleocurrent records thus suggests a potential link between AAIW bottom current strength and Southern Hemisphere climate changes (Fig. 4D).

The long-term increase in AAIW circulation correlates to Holocene cooling (~2 °C) and freshening in the Southern Hemisphere recorded in ice cores around Antarctica (Masson et al., 2000) that show a widespread early Holocene thermal maximum (HTM) followed by cooler and more glaciated conditions. The HTM and the subsequent cooling is known from various terrestrial and marine records from the Southern Hemisphere (Mayewski et al., 2004; Wanner et al., 2011b; Bostock et al., 2013). Accordingly, variations in sea surface temperature records from the southeast Pacific (Shevenell et al., 2011) (Fig. 4F) show a decreasing trend (2–4 °C) over the course of the Holocene indicating a substantial Southern Ocean surface water cooling. Such upper ocean cooling in the AAIW source region would decrease the vertical stratification leading to increased winter convection, formation rate volume of AAIW (Sloyan and Rintoul, 2001).

Intermediate water temperature records between 600 and 900 m from the eastern equatorial Pacific, a region partly influenced by AAIW, indeed indicate an early Holocene warmth and subsequent cooling at intermediate depths which suggest a direct response to Southern Hemisphere climate changes (Rosenthal et al., 2013) (Fig. 4E). Rosenthal et al. (2013) show that water masses linked to Antarctic intermediate waters were warmer by 1.5 ± 0.4 °C during the HTM than over the late Holocene. The cooling trend at intermediate depths must thereby have been largely compensated by freshening at the Southern Hemisphere high-latitude AAIW source regions as the density of AAIW remained relatively constant throughout the Holocene (Rosenthal et al., 2013). Given that intermediate water temperature records are very sparse for the Holocene, the IWT records from the eastern equatorial Pacific gives support for our suggestion that long-term Holocene cooling in the high-latitude Southern Hemisphere might had an impact on the circulation, renewal, and modification of AAIW (Sloyan and Rintoul, 2001).

A change in AAIW renewal might be further indicated by the increased influence of more corrosive AAIW/UCDW at the expense of NADW at ~2 km (Fig. 3C) which most probably reflects a slight deepening of the interface between southern- and northern source waters over last 5.5 kyr (Fig. 5). Considering no significant changes in intermediate water density throughout the Holocene (as reconstructed in the eastern equatorial Pacific (Rosenthal et al., 2013)), we assume that the expansion and deepening of the lower limit of AAIW/UCDW indicates indeed a significant increase in AAIW volume and possibly transport (Fig. 5). That would suggest that the increase in AAIW volume is accompanied by an increase in AAIW flux, thereby supporting a significant change in AAIW circulation and renewal from mid-to late Holocene most probably in response to the insolation-related Southern Hemisphere winter-spring cooling trend. However, any conclusive statement concerning perturbations in AAIW source regions remains speculative because our paleocurrent record reflect changes in AAIW bottom current strength, but not in AAIW temperature or salinity.

Thus, although there is agreement that perturbations in AAIW strength are in some way associated with high-latitude Southern Hemisphere climate change (Fig. 4), there is still not a consensus on the precise mechanism(s) causing AAIW variability. Further work is therefore required to produce high resolution Holocene records at intermediate water depths and to determine the role of Southern Hemisphere climate changes in driving changes in the formation rate, characteristics and circulation of AAIW.

5.2. Implication of Holocene AAIW variability

Today, the formation of NADW in the high latitudes of the North Atlantic is fed by AAIW and, in part, by upper-thermocline water (Rintoul, 1991). AAIW supplies a large fraction of the northward flow required to balance the southward export of NADW, and thus represents an active player in the AMOC (Lumpkin and Speer, 2007). However, a potential AAIW-NADW linkage during the Holocene is poorly understood due to sparsity of accurately dated marine archives with sub-millennial-scale resolution. By investigating a North Atlantic paleocurrent record (NEAP15K), Bianchi and McCave (1999) reported Holocene oscillations in the strength of the ISOW, that significantly contributes to the formation of NADW, thus suggesting short-term changes in the AMOC during the Holocene. An even higher temporal resolution Holocene paleocurrent record from the North Atlantic (NEAP4K) (Hall et al., 2004) (Fig. 4A) allows the detection of extensive sub-millennial-scale variability superimposed on the millennial-scale Holocene oscillations in the strengths of the ISOW recorded in NEAP15K (Bianchi and McCave, 1999). Interestingly, a comparison of the GeoB13862-1 $mean_{(SS)}$ with the NEAP4K $mean_{(SS)}$ record (Fig. 4A,B) highlights a strong similarity not only in the longer-term trends as well as in some of the key sub-millennial features of both records. The observed changes in the bottom current strength of AAIW (Fig. 4B) are antiphased with perturbations in NADW circulation (Fig. 4A): periods of increased AAIW advection correlate with periods of reduced NADW bottom current strength and vice versa. The most notable examples occur at ~ 8.5–9.0, 8.0, 5.0, 3.5 and 2.5 ka BP. The inverse relationship between

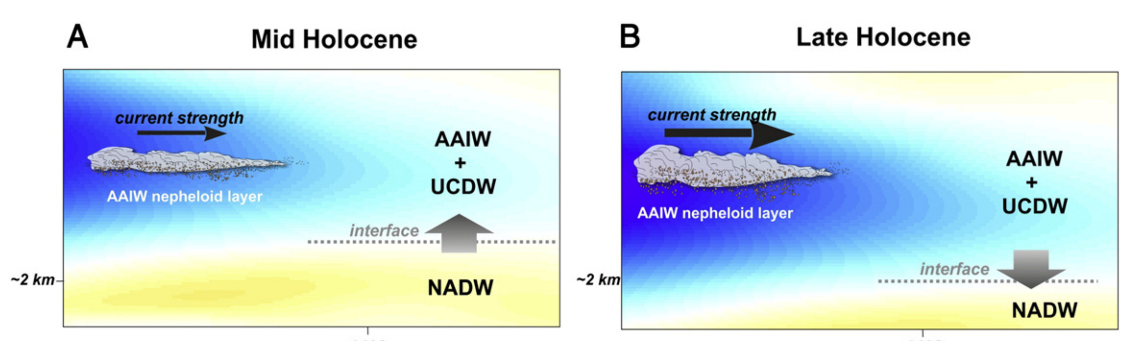

Fig. 5. Schematic vertical section of water mass distribution in the Southwest Atlantic during (A) mid- and (B) late Holocene. The increase in AAIW strength and the deepening and expansion of the AAIW + UCDW suggest a significant increase in AAIW volume transport after ~7 ka BP most probably related to cooling and freshening in AAIW source regions. AAIW – Antarctic Intermediate Water; NADW – North Atlantic Deep Water; UCDW – Upper Circumpolar Deep Water.

sub-millennial-scale variability in AAIW and in NADW flow intensity provides strong evidence for an AAIW-NADW see-saw operating during the Holocene.

Model simulations demonstrate a pervasive link between the formation of AAIW and NADW for Holocene boundary conditions (Graham et al., 2011), and highlight the possibility that initial changes in AMOC strength can be related to perturbations in AAIW. Graham et al. (2011) show that incursions of anomalously cold and fresh AAIW into the upper water column of the North Atlantic can lead to a cooling and freshening of the North Atlantic, thereby contributing to the reduction of NADW formation. The ventilation timescale for AAIW in the Atlantic is 50–150 years (Holzer et al., 2010) supports the hypothesis of a quasi-synchronous AAIW-NADW coupling. We therefore consider that enhanced incursions of cool and fresh AAIW into the North Atlantic could have had a weakening effect on the formation of NADW during the Holocene. Thereby, incursions of cool and fresh AAIW into the upper water column of the North Atlantic may have cooled and freshened the North Atlantic, contributing to the reduction of NADW formation. Accordingly, we suggest that relatively small perturbations in AAIW circulation and renewal during the Holocene are efficiently transferred to the North Atlantic where they have significant effects on the AMOC. The correspondence of sub-millennial-scale variability in Southwest- and North Atlantic paleocurrent records suggests a direct linkage between intermediate water variability in the Southern Hemisphere and AMOC variations. This implies that AAIW and North Atlantic deep ocean fluctuations during the course of the Holocene appear to be essentially synchronous which underscore the potential connection between the Southern Ocean and the North Atlantic in the absence of large ice sheets.

6. Conclusions

Here we present a high temporal resolution Holocene paleocurrent record from the Southwest Atlantic that documents a highly variable intermediate water circulation throughout the Holocene. Superimposed on a slight increase in AAIW bottom current strength at ~7 ka BP, a succession of millennial-scale AAIW variations is recognized in our paleocurrent record. Our data indicates that abruptly increased AAIW northward advection was associated with periods of reduced NADW strength and vice versa. The inverse relationship of millennial-scale changes in the northward penetration of AAIW and NADW formation provide strong evidence for a AAIW-NADW see-saw operating during the Holocene. We therefore suggest that even small changes of AAIW may cause substantial AMOC variations and therefore could be an additional source of climate variability. However, although a change in AMOC in response to dynamical processes in the Southern Ocean seems a possible scenario, it still relies on mostly indirect inferences. Continuing research is therefore encouraged to evaluate Holocene history of the deep- and intermediate water circulation in the Atlantic Ocean.

Acknowledgments

We thank the two Reviewers for their thorough and constructive comments that improved the manuscript. We thank T. Töpfer who kindly agreed to contribute unpublished BDX data derived from his unpublished BSc thesis performed under supervision of R. Henrich. We also thank G. Martínez Méndez and J. Groeneveld for comments and discussion. This study was funded through the DFG-Research Center/Cluster of Excellence "The Ocean in the Earth System" and was supported by GLOMAR – Bremen International Graduate School for Marine Sciences. CMC acknowledges the support from FAPESP (grant 2012/17517-3) and CAPES (grants 1976/2014 and 564/2015). ARP acknowledges the support of grant CRN3070 from the Inter-American Institute for Global Change Research (US NSF grant GEO-1128040). The data of this study are available in the PANGAEA database.

References

Arz, H., Gerhardt, S., Pätzold, J., Röhl, U., 2001. Millennial-scale changes of surface-and deep-water flow in the western tropical Atlantic linked to Northern Hemisphere high-latitude climate during the Holocene. Geology 29, 239–242.

Berger, A., Loutre, M.F., 1991. Insolation values for the climate of the last 10 million years. Quat. Sci. Rev. 10 (4), 297–317. http://dx.doi.org/10.1016/0277-3791(91)90033-Q.

Bianchi, G.G., McCave, I.N., 1999. Holocene periodicity in North Atlantic climate and deep-ocean flow south of Iceland. Nature 397 (6719), 515–517.

Bond, G., Kromer, B., Beer, J., Muscheler, R., Evans, M.N., Showers, W., Hoffmann, S., Lotti-Bond, R., Hajdas, I., Bonani, G., 2001. Persistent solar influence on North Atlantic climate during the Holocene. Science 294 (5549), 2130–2136. http://dx.doi.org/10.1126/science.1065680.

Bostock, H.C., et al., 2013. A review of the Australian-New Zealand sector of the Southern Ocean over the last 30 ka (Aus-INTIMATE project). Quat. Sci. Rev. 74, 35–57. http://dx.doi.org/10.1016/j.quascirev.2012.07.018.

Bozzano, G., Violante, R.A., Cerredo, M.E., 2011. Middle slope contourite deposits and associated sedimentary facies off NE Argentina. Geo-Marine Lett. 31 (5–6), 495–507. http://dx.doi.org/10.1007/s00367-011-0239-x.

Came, R.E., Oppo, D.W., Curry, W.B., Lynch-Stieglitz, J., 2008. Deglacial variability in the surface return flow of the Atlantic meridional overturning circulation. Paleoceanography 23 (1), PA1217. http://dx.doi.org/10.1029/2007PA001450.

Emerson, S.R., Archer, D., 1990. Calcium carbonate preservation in the ocean. Philos. Trans. R. Soc. London. Ser. A, Math. Phys. Sci. 331 (1616), 29–40.

Fletcher, M.-S., Moreno, P.I., 2012. Have the Southern Westerlies changed in a zonally symmetric manner over the last 14,000 years? A hemisphere-wide take on a controversial problem. Quat. Int. 253, 32–46. http://dx.doi.org/10.1016/j.quaint.2011.04.042.

Garabato, N.A.C., Jullion, L., Stevens, D.P., Heywood, K.J., King, B.A., 2009. Variability of subantarctic mode water and Antarctic Intermediate Water in the Drake Passage during the late-twentieth and early-twenty-first centuries. J. Clim. 22 (13), 3661–3688. http://dx.doi.org/10.1175/2009JCLI2621.1.

Goossens, D., 2008. Techniques to measure grain-size distributions of loamy sediments: a comparative study of ten instruments for wet analysis. Sedimentology 55 (1), 65–96. http://dx.doi.org/10.1111/j.1365-3091.2007.00893.x.

Graham, J.A., Stevens, D.P., Heywood, K.J., Wang, Z., 2011. North Atlantic climate responses to perturbations in Antarctic Intermediate Water. Clim. Dyn. 37 (1–2), 297–311. http://dx.doi.org/10.1007/s00382-010-0981-1.

Gwilliam, C.S., 1996. Modelling the global ocean circulation on the T3D. In: Ecer, A., Periaux, J., Satofuka, N., Taylor, S. (Eds.), Parallel Computational Fluid Dynamics 1995, pp. 33–40 North-Holland, Amsterdam.

Hall, I.R., Bianchi, G.G., Evans, J.R., 2004. Centennial to millennial scale Holocene climate-deep water linkage in the North Atlantic. Quat. Sci. Rev. 23 (14–15), 1529–1536. http://dx.doi.org/10.1016/j.quascirev.2004.04.004.

Henrich, R., Baumann, K.-H., Gerhardt, S., Gröger, M., Volbers, A., 2004. Carbonate Preservation in Deep and Intermediate Water Masses in the South Atlantic: Evaluation and Geological Record (a Review). In: Wefer, G., Mulitza, S., Ratmeyer, V. (Eds.), The South Atlantic in the Late Quaternary SE - 28. Springer, Berlin Heidelberg, pp. 645–670.

Hernandez-Molina, F.J., Paterlini, M., Violante, R., Marshall, P., de Isasi, M., Somoza, L., Rebesco, M., 2009. Contourite depositional system on the Argentine Slope: an exceptional record of the influence of Antarctic water masses. Geology 37 (6), 507–510. http://dx.doi.org/10.1130/G25578A.1.

Holzer, M., Primeau, F.W., Smethie, W.M., Khatiwala, S., 2010. Where and how long ago was water in the western North Atlantic ventilated? Maximum entropy inversions of bottle data from WOCE line A20. J. Geophys. Res. 115 (C7), C07005. http://dx.doi.org/10.1029/2009JC005750.

Huang, K.F., Oppo, D.W., Curry, W.B., 2014. Decreased influence of Antarctic intermediate water in the tropical Atlantic during North Atlantic cold events. Earth Planet. Sci. Lett. 389, 200–208. http://dx.doi.org/10.1016/j.epsl.2013.12.037.

Jahnke, R.A., Craven, D.B., 1994. The influence of organic matter diagenesis on $CaCO_3$ dissolution at the deep-sea floor. Science 58 (13), 2799–2809.

Jonkers, L., Prins, M.A., Brummer, G.J.A., Konert, M., Lougheed, B.C., 2009. Experimental insights into laser diffraction particle sizing of fine-grained sediments for use in palaeoceanography. Sedimentology 56 (7), 2192–2206. http://dx.doi.org/10.1111/j.1365-3091.2009.01075.x.

Kilian, R., Lamy, F., 2012. A review of Glacial and Holocene paleoclimate records from southernmost Patagonia (49–55°S). Quat. Sci. Rev. 53, 1–23. http://dx.doi.org/10.1016/j.quascirev.2012.07.017.

Krastel, S., Wefer, G., Hanebuth, T.J.J., Antobreh, A.A., Freudenthal, T., Preu, B., Schwenk, T., Strasser, M., Violante, R., Winkelmann, D., 2011. Sediment dynamics and geohazards off Uruguay and the de la Plata River region (northern Argentina and Uruguay). Geo-Marine Lett. 31 (4), 271–283. http://dx.doi.org/10.1007/s00367-011-0232-4.

Krastel, S., et al., 2012. Preliminary results of RV METEOR Cruise M78/3. Sediment transport off Uruguay and Argentina: from the shelf to the deep sea; 19.05. 2009–06.07. 2009, Montevideo. Berichte Fachbereich Geowissenschaften 285, 79.

Lumpkin, R., Garzoli, S., 2011. Interannual to decadal changes in the western South Atlantic's surface circulation. J. Geophys. Res. 116 (C1), C01014. http://dx.doi.org/10.1029/2010JC006285.

Lumpkin, R., Speer, K., 2007. Global Ocean meridional overturning. J. Phys. Oceanogr. 37 (10), 2550–2562. http://dx.doi.org/10.1175/JPO3130.1.

Marchitto, T., Curry, W., Oppo, D., 1998. Millennial-scale changes in North Atlantic circulation since the last glaciation. Nature 393 (June), 557–561.

Masson, V., et al., 2000. Holocene climate variability in Antarctica based on 11 ice-Core isotopic records. Quat. Res. 54 (3), 348–358. http://dx.doi.org/10.1006/qres.2000.2172.

Mayewski, P.A., et al., 2004. Holocene climate variability. Quat. Res. 62 (3), 243–255. http://dx.doi.org/10.1016/j.yqres.2004.07.001.
McCave, I., Manighetti, B., Robinson, S., 1995. Sortable silt and fine sediment size/composition slicing: parameters for palaeocurrent speed and palaeoceanography. Paleoceanography 10 (3), 593–610.
McCave, I.N., Hall, I.R., Bianchi, G.G., 2006. Laser vs. settling velocity differences in silt grainsize measurements: Estimation of palaeocurrent vigour. Sedimentology 53 (4), 919–928. http://dx.doi.org/10.1111/j.1365-3091.2006.00783.x.
Mulitza, S., Prange, M., Stuut, J.-B., Zabel, M., von Dobeneck, T., Itambi, A.C., Nizou, J., Schulz, M., Wefer, G., 2008. Sahel megadroughts triggered by glacial slowdowns of Atlantic meridional overturning. Paleoceanography 23 (4), PA4206. http://dx.doi.org/10.1029/2008PA001637.
Oke, P., England, M., 2004. Oceanic response to changes in the latitude of the Southern Hemisphere subpolar westerly winds. J. Clim. 17, 1040–1054.
Pahnke, K., Goldstein, S.L., Hemming, S.R., 2008. Abrupt changes in Antarctic Intermediate Water circulation over the past 25,000 years. Nat. Geosci. 1 (12), 870–874. http://dx.doi.org/10.1038/ngeo360.
Peterson, R., Stramma, L., 1991. Upper-level circulation in the South Atlantic Ocean. Prog. Oceanogr. 26, 1–73.
Piola, A., Gordon, A., 1989. Intermediate waters in the southwest South Atlantic. Deep-Sea Res. 36 (1), 1–16. http://dx.doi.org/10.1016/0198-0149(89)90015-0.
Piola, A., Matano, R., 2001. In: JH, T.S.S. (Ed.), Brazil and Falklands (Malvinas) currents. Academic Press, pp. 340–349 Encycloped.
Preu, B., Hernández-Molina, F.J., Violante, R., Piola, A.R., Paterlini, C.M., Schwenk, T., Voigt, I., Krastel, S., Spiess, V., 2013. Morphosedimentary and hydrographic features of the northern Argentine margin: the interplay between erosive, depositional and gravitational processes and its conceptual implications. Deep Sea Res. Part I Oceanogr. Res. Pap. 75, 157–174. http://dx.doi.org/10.1016/j.dsr.2012.12.013.
Reimer, P., Baillie, M., Bard, E., 2009. IntCal09 and Marine09 radiocarbon age calibration curves, 0–50,000 years cal BP. Radiocarbon 51, 1111–1150.
Renssen, H., Goosse, H., Fichefet, T., Masson-Delmotte, V., Koç, N., 2005. Holocene climate evolution in the high-latitude Southern Hemisphere simulated by a coupled atmosphere–sea ice–ocean–vegetation model. The Holocene 15 (7), 951–964. http://dx.doi.org/10.1191/0959683605hl869ra.
Ribbe, J., 2001. Intermediate water mass production controlled by Southern Hemisphere winds. Geophys. Res. Lett. 28 (3), 535–538.
Rickaby, R.E.M., Elderfield, H., 2005. Evidence from the high-latitude North Atlantic for variations in Antarctic Intermediate Water flow during the last deglaciation. Geochem. Geophys. Geosyst. 6 (5), Q05001. http://dx.doi.org/10.1029/2004GC000858.
Rintoul, S.R., 1991. South Atlantic interbasin exchange. J. Geophys. Res. 96 (C2), 2675–2692. http://dx.doi.org/10.1029/90JC02422.
Rosenthal, Y., Linsley, B.K., Oppo, D.W., 2013. Pacific Ocean heat content during the past 10,000 years. Science 342 (6158), 617–621. http://dx.doi.org/10.1126/science.1240837.
Saenko, O.A., Weaver, A.J., 2001. Importance of wind-driven sea ice motion for the formation of Antarctic Intermediate Water in a global climate model. Geophys. Res. Lett. 28 (21), 4147–4150. http://dx.doi.org/10.1029/2001GL013632.
Shanmugam, G., 2003. Deep-marine tidal bottom currents and their reworked sands in modern and ancient submarine canyons. Mar. Pet. Geol. 20 (5), 471–491. http://dx.doi.org/10.1016/S0264-8172(03)00063-1.
Shevenell, A.E., Ingalls, A.E., Domack, E.W., Kelly, C., 2011. Holocene Southern Ocean surface temperature variability west of the Antarctic Peninsula. Nature 470 (7333), 250–254. http://dx.doi.org/10.1038/nature09751.
Sijp, W.P., England, M.H., 2008. The effect of a northward shift in the southern hemisphere westerlies on the global ocean. Prog. Oceanogr. 79 (1), 1–19. http://dx.doi.org/10.1016/j.pocean.2008.07.002.
Sloyan, B.M., Rintoul, S.R., 2001. Circulation, renewal, and modification of Antarctic mode and Intermediate Water*. J. Phys. Oceanogr. 31 (4), 1005–1030. http://dx.doi.org/10.1175/1520-0485(2001)031<1005:CRAMOA>2.0.CO;2.
Stramma, L., England, M., 1999. On the water masses and mean circulation of the South Atlantic Ocean. J. Geophys. Res. 104.
Stuiver, M., Reimer, P., 1993. Extended (super 14) C data base and revised CALIB 3.0 (super 14) C age calibration program. Radiocarbon 35, 215–230.
Thornalley, D.J.R., Barker, S., Broecker, W.S., Elderfield, H., McCave, I.N., 2011. The deglacial evolution of North Atlantic deep convection. Science 331 (6014), 202–205. http://dx.doi.org/10.1126/science.1196812.
Voigt, I., Henrich, R., Preu, B., Piola, A., Hanebuth, T.J.J., Tillmann, S., Chiessi, C.M., 2013. A submarine canyon as a climate archive-interaction of the Antarctic Intermediate Water with the Mar del Plata Canyon (Southwest Atlantic). Mar. Geol. 341, 46–57. http://dx.doi.org/10.1016/j.margeo.2013.05.002.
Voigt, I., Chiessi, C.M., Prange, M., Mulitza, S., Groeneveld, J., Varma, V., Henrich, R., 2015. Holocene shifts of the southern westerlies across the South Atlantic. Paleoceanography 30, 39–51. http://dx.doi.org/10.1080/00358536408452524.
Volbers, A.N.A., Henrich, R., 2002. Late Quaternary variations in calcium carbonate preservation of deep-sea sediments in the northern Cape Basin: results from a multiproxy approach. Mar. Geol. 180 (1–4), 203–220. http://dx.doi.org/10.1016/S0025-3227(01)00214-6.
Wanner, H., Solomina, O., Grosjean, M., Ritz, S.P., Jetel, M., 2011a. Structure and origin of Holocene cold events. Quat. Sci. Rev. 30 (21–22), 3109–3123. http://dx.doi.org/10.1016/j.quascirev.2011.07.010.
Wanner, H., Solomina, O., Grosjean, M., Ritz, S.P., Jetel, M., 2011b. Structure and origin of Holocene cold events. Quat. Sci. Rev. 30 (21–22), 3109–3123. http://dx.doi.org/10.1016/j.quascirev.2011.07.010.
Wunsch, C., 2000. On sharp spectral lines in the climate record and the millennial peak. Paleoceanography 15 (4), 417–424. http://dx.doi.org/10.1029/1999PA000468.
Xie, R.C., Marcantonio, F., Schmidt, M.W., 2012. Deglacial variability of Antarctic Intermediate Water penetration into the North Atlantic from authigenic neodymium isotope ratios. Paleoceanography 27 (3), PA3221. http://dx.doi.org/10.1029/2012PA002337.
Zahn, R., Stüber, A., 2002. Suborbital intermediate water variability inferred from paired benthic foraminiferal Cd/Ca and N13C in the tropical West Atlantic and linking with North Atlantic climates. Earth Planet. Sci. Lett. 200 (200), 191–205.